Optimization of Active Layer Morphology by Small Molecule Donor Design Enables over 15% Efficiency in Small-Molecule Solar Cells

Cunbin An,[a] Yunpeng Qin,[c] Tao Zhang,[a] Qianglong Lv,[a] Jinzhao Qin,[ab] Shaoqing Zhang,[a] Chang He,[a] Harald Ade,[c] and Jianhui Hou*[ab]

[a]Beijing National Laboratory for Molecular Sciences, State Key Laboratory of Polymer Physics and Chemistry, Institute of Chemistry, Chinese Academy of Sciences, Beijing 100190, China. E-mail: hjhzlz@iccas.ac.cn; Tel.: +86-10-82615900.

[b]University of Chinese Academy of Sciences, Beijing 100049, China.

[c]Department of Physics, North Carolina State University, Raleigh, NC 27695, USA

Table of Contents

1. Instruments and Measurements

^{1}H NMR and ^{13}C NMR spectra were measured in deuterated solvents on a Bruker AVANCE 300 MHz or 400 MHz NMR spectrometer at room temperature. Thermogravimetric analysis (TGA) measurements were carried out on TGA-2050 Thermogravimetry Analyze. The differential scanning calorimetry (DSC) measurements were performed on TA instruments-Waters LLC. The current density−voltage *J*−*V* measurements were performed by using the solar simulator (SS-F5-3A, Enlitech) along with AM 1.5G spectra (100 mW/cm^2). The power conversion efficiencies of the organic solar cells were measured under 1 sun, AM 1.5G (air mass 1.5 global) (100 mW/cm^2), using a XES-70S1 (SAN-EI ELECTRIC CO., Ltd.) solar simulator (AAA grade, 70 mm ×70 mm photobeam size). The EQE spectra were measured through the Solar Cell Spectral Response Measurement System QE-R3011 (Enli Technology Co., Ltd., Taiwan). The light intensity at each wavelength was calibrated with a standard single-crystal Si photovoltaic cell.

Optical characterizations: UV-vis absorption spectra of materials in solution and in solid thin films were measured on a Hitachi U-3100 UV−vis spectrophotometer. The solid thin film samples were spin-coated onto quartz plates (1×1 cm^2).

Cyclic Voltammetry (CV): The electrochemical cyclic voltammetry was measured on a CH1650D electrochemical workstation in a three-electrode cell in anhydrous acetonitrile solvents solution of Bu_4NPF_6 (0.1 M) with a scan rate of 50 mV/s at room temperature under argon. A Ag/Ag$^+$ wire, A platinum wire, and a glassy carbon electrode were used as the reference electrode counter electrode, and working electrode, respectively. The potential of Ag/Ag$^+$ reference electrode was calibrated by using ferrocene/ferroncenium (Fc/Fc$^+$) as the redox couple.

Exciton dissociation, charge carrier mobility, and photo-CELIV measurements. Exciton dissociation and photo-CELIV mobility data were obtained by the all-in-one characterization platform, Paios (FluximAG, Switzerland). In J_{ph}-V_{eff} curve, J_{ph} is given by $J_{ph} = J_L - J_D$, where J_L and J_D are current densities for illumination and dark conditions, respectively. The V_{eff} is defined as $V_{eff} = V_0 - V$, where V_0 is voltage when the J_{ph} is zero, V is the applied voltage. The J_{sat} is the saturation photocurrent density. In photo-CELIV transient method, all the transient measurements were recorded by applying a 0.32 V/μs linearly increasing reverse bias pulse with 80 μs delay time.

Highly sensitive EQE and EQE_{EL} measurements. Highly sensitive EQE was measured using a integrated system (PECT-600, Enlitech), where the photocurrent was amplified and modulated by

a lock-in instrument. EQE_{EL} measurements were performed by applying external voltage/current sources through the devices (ELCT-3010, Enlitech). All of the devices were prepared for EQE_{EL} measurements according to the optimal device fabrication conditions. EQE_{EL} measurements were carried out from 0 to 4 V.

GIWAXS measurements were performed at beamline 7.3.362 at the Advanced Light Source (ALS) in Lawrence Berkeley National Lab, Berkeley, CA. The precise sample-to-detector distance was determined with a silver behenate (AgB) standard. The samples were measured in a helium environment to minimize air scattering using a 10 keV energy X-ray beam, which was incident at a grazing angle of 0.13°. The scattered Xrays were detected using a Dectris Pilatus 2 M photon counting detector. RSoXS measurements were performed at beamline 11.0.1.2 at ALS. The 2D X-ray data were reduced and analyzed with a modified NIKA81 package.

Photovoltaic device fabrication and testing: All devices were fabricated with the conventional device architecture of ITO/poly(3,4-ethylenedioxythiophene):poly(styrenesulfonate) (PEDOT:PSS)/BHJ/PFN-Br/Al. Pre-patterned indium tin oxide (ITO)-coated glass was cleaned sequential sonication in deionized water, acetone and isopropanol twice for 15 min. Then it was transferred to oven and dried at 150 °C for 15 min. After ultraviolet-ozone treatment for 20 min, the 10 nm layer of PEDOT:PSS (Heraeus Materials, 4083) was spin-coated on ITO. The substrates were annealed for 15 min at 150 °C, and transferred to the nitrogen-filled glovebox. The active layer materials were dissolved in chloroform with a concentration of 10 mg/mL. The solution need to be heated at 40 ^{o}C until total dissolution. The active layers were spin-coated onto PEDOT:PSS modified substrate. The film thickness was controlled at around 100 nm by tuning the spin-coating speed. The thickness was measured via the surface profilometer (Bruker Dektak XT). Finally, PFN-Br was spin-coated (3000rpm, 30s) onto the active laye as the cathode buffer layer, and the whole device was completed by vacuum evaporating Al metal electrodes (100 nm) to acquire an area of 4 mm^2 cell. Device *J–V* characteristics were measured under 100 mW cm^{-2} of the standard AM 1.5G spectrum.

Carrier mobility measurement: The carrier mobility of the blend films were measured using the SCLC method, with the hole-only and electron-only device architecture of ITO/PEDOT:PSS/BHJ/Au and ITO/ZnO/BHJ/Al, respectively.

AFM characterizations: All film samples were prepared using spin-coating onto ITO/PEDOT:PSS substrates. The measurements were carried out by a Nanoscope V (Vecco) IN tapping mode.

Density functional theory (DFT) calculation: The molecular modeling calculations were conducted using the Gaussian 09 program based on the density functional theory method using B3LYP/6-31G (d, p) level.

2. Synthetic detail

5'',5''''-(4,8-bis(5-((2-ethylhexyl)thio)-4-fluorothiophen-2-yl)benzo[1,2-b:4,5-b']dithiophene-2,6-diyl)bis(3',3''-dihexyl-[2,2':5',2''-terthiophene]-5-carbaldehyde) **(3a)**

Distannyl compound **1a** (903.7 mg, 0.8 mmol), compound **2** (921.6 mg, 1.76 mmol) and $Pd(PPh_3)_4$ (28 mg) were dissolved into 50 mL of dry toluene. The reaction mixture was refluxed 16 hours. Afterwards, the solvent was removed by rotary evaporator, the crude product was purified by silica gel column chromatography to give the product of **3a** with a high yield of 91% (1.14 g, red solid). ^{1}H NMR (400 MHz,$CDCl_3$), δ 9.85 (s, 2H), 7.66 (t, *J* = 4.0Hz, 2H), 7.47 (br, 2H), 7.18 (br, 4H), 7.03 (s, 2H), 6.97 (d, *J* = 4.0Hz, 2H), 2.96 (d, *J* = 8.0Hz, 4H), 2.80 (m, 8H) 1.68–1.34 (m, 50H), 0.99-0.89 (m, 24H); ^{13}C NMR (100 MHz, $CDCl_3$) δ 182.55, 160.57, 157.10, 146.03, 142.61,142.25, 141.13, 139.17, 138.45, 137.06, 136.91, 135.86, 134.69, 131.16, 129.76, 129.06, 128.78, 125.83, 122.37, 118.02, 115.39, 115.13, 42.96, 39.57, 32.17, 31.80, 30.41, 30.34, 29.99, 29.90, 29.51, 29.46, 28.92, 25.47, 23.09, 22.77, 14.29, 14.25, 14.22, 11.05. MS (MALDI-TOF, C84H100F2O2S12, m/z): 1562.84.

(5Z,5'Z)-5,5'-(((4,8-bis(5-((2-ethylhexyl)thio)-4-fluorothiophen-2-yl)benzo[1,2-b:4,5-b']dithiophene-2,6-diyl)bis(3',3''-dihexyl-[2,2':5',2''-terthiophene]-5'',5-diyl))bis(methanylylidene))bis(3-butyl-2-thioxothiazolidin-4-one) **(B3T-T)**

Compound **3a** (312.8 mg, 0.2 mmol) and 3-butyl-2-thioxothiazolidin-4-one **4** (378.6 mg, 2 mmol) were dissolved into 20 mL of dry chloroform under Agron protect. Next, the 0.1 mL of piperidine was added into above solution. The reaction mixture was refluxed overnight. The reaction mixture was poured into water and extracted with chloroform (3x20 mL). The organic layers were combined, dried with $MgSO_4$ and filtered. The filtrate was concentrated and purified by silica gel column chromatography to give the product of **B3T-T** with a yield of 85% (324.2 mg, red solid). ^{1}H NMR (400 MHz,$CDCl_3$), δ 7.70 (s, 2H), 7.35 (2H), 7.23 (2H), 7.18 (2H), 7.08 (2H), 6.94-6.89 (4H), 4.03 (4H), 2.99 (d, *J* = 8.0Hz, 4H), 2.73 (m, 8H), 1.66–1.26 (m, 58H), 1.01-0.84 (m, 30H); ^{13}C NMR (100 MHz, $CDCl_3$) δ 192.13, 167.51, 160.16, 157.56, 144.27, 141.93, 140.91, 139.33, 139.24, 138.45, 138.34, 137.07, 135.49, 134.53, 129.05, 128.75, 126.38, 124.81, 122.33, 120.35, 118.53, 118.27, 117.94, 115.42, 115.23, 44.74, 43.04, 39.67, 32.26, 31.89, 31.86, 30.39, 30.15, 30.01, 29.85, 29.57, 2918, 28.98, 25.56, 23.13, 22.86, 22.82, 20.23, 14.29, 14.29, 13.80, 11.11. MS (MALDI-TOF, C98H118F2N2O2S10, m/z): 1905.99.

5'',5''''-(4,8-bis(3-((2-ethylhexyl)thio)phenyl)benzo[1,2-b:4,5-b']dithiophene-2,6-diyl)bis(3',3''-dihexyl-[2,2':5',2''-terthiophene]-5-carbaldehyde) (**3b**)

Distannyl compound **1b** (765.3 g, 0.8 mmol), compound **2** (921.6 g, 1.76 mmol) and $Pd(PPh_3)_4$ (28 mg) were dissolved into 50 mL of dry toluene. The reaction mixture was refluxed 15 hours. Afterwards, the solvent was removed by rotary evaporator, the crude product was purified by silica gel column chromatography to give the product of **3b** with a high yield of 90% (1.09 g, red solid).^{1}H

NMR (400 MHz,$CDCl_3$), δ 9.88 (s, 2H), 7.70 (d, *J* = 4.0Hz, 2H), 7.66 (br, 2H), 7.53-7.47 (br, 6H), 7.30 (s, 2H), 7.22 (d, *J* = 4.0Hz, 2H), 7.06 (s, 2H), 6.99 (s, 2H), 3.03 (d, *J* = 8.0Hz, 4H), 2.83 (m, 8H), 1.73–1.28 (m, 50H), 0.95-0.83 (m, 24H); ^{13}C NMR (100 MHz, $CDCl_3$) δ 182.66, 146.16, 142.67, 142.33, 141.25,139.58, 139.24, 138.00, 137.73, 137.08, 136.96, 136.04, 135.52, 130.53, 129.65, 129. 61, 129.56, 129.17, 128.80, 128.57, 128.50, 126.38, 125.99, 118.57, 39.11, 37.97, 32.57, 31.78, 31.77, 30.47, 30.35, 29.91, 29.79, 29.40, 29.39, 28.92, 25.84, 23.12, 22.73, 14.22, 14.21, 14.20, 10.98. MS (MALDI-TOF,C88H106O2S10, m/z): 1514.96.

(5Z,5'Z)-5,5'-(((4,8-bis(3-((2-ethylhexyl)thio)phenyl)benzo[1,2-b:4,5-b']dithiophene-2,6-diyl)bis(3',3''-dihexyl-[2,2':5',2''-terthiophene]-5'',5-diyl))bis(methanylylidene))bis(3-butyl-2-thioxothiazolidin-4-one) **(B3T-P)**

Compound **3a** (303.3 mg, 0.2 mmol) and 3-butyl-2-thioxothiazolidin-4-one **4** (378.6 mg, 2 mmol) were dissolved into 20 mL of dry chloroform under Agron protect. Next, the 0.1 mL of piperidine was added into above solution. The reaction mixture was refluxed overnight. The reaction mixture was poured into water and extracted with chloroform (3x20 mL). The organic layers were combined, dried with $MgSO_4$ and filtered. The filtrate was concentrated and purified by silica gel column chromatography to give the product of **B3T-P** with a yield of 83% (308.6 mg, red solid). ^{1}H NMR (400 MHz,$CDCl_3$), δ 7.83 (s, 2H), 7.66 (2H), 7.51 (br, 6H), 7.18 (2H), 7.35 (d, *J* = 8.0Hz, 2H), 7.29 (s, 2H), 7.19 (d, *J* = 8.0Hz, 2H), 7.05 (s, 2H), 6.97 (s, 2H), 4.13 (t, *J* = 8.0Hz,4H), 3.03 (d, *J* = 8.0Hz, 4H), 2.82 (m, 8H), 1.71–1.30 (m, 58H), 0.98-0.86 (m, 30H); ^{13}C NMR (100 MHz, $CDCl_3$) δ 192.30, 167.65, 144.38, 142.07, 141.13, 139.61, 139.25, 138.01, 137.72, 137.25, 137.09, 135.72, 135.45, 134.75, 130.69, 129.86, 129.57, 129.17, 128.90, 128.61, 128.50, 126.67, 126.44, 125.06, 120.42, 118.54, 44.79, 39.17, 38.07, 32.61, 31.84, 31.80, 30.43, 30.00, 29.85, 29.46, 29.43, 29.21, 28.95,

25.88, 23.14, 22.80, 22.75, 20.23, 14.26, 14.25,14.20, 13.83, 11.01. MS (MALDI-TOF, C102H124N2O2S14, m/z): 1858.10

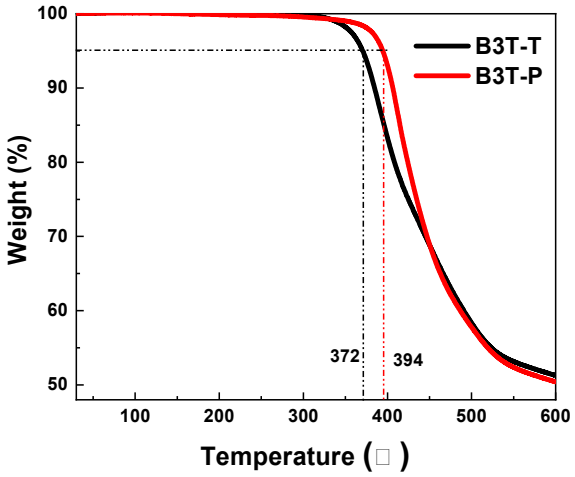

Figure S1. TGA curves of **B3T-T** and **B3T-P** at a heating rate of 10 ºC min^{-1} under nitrogen.

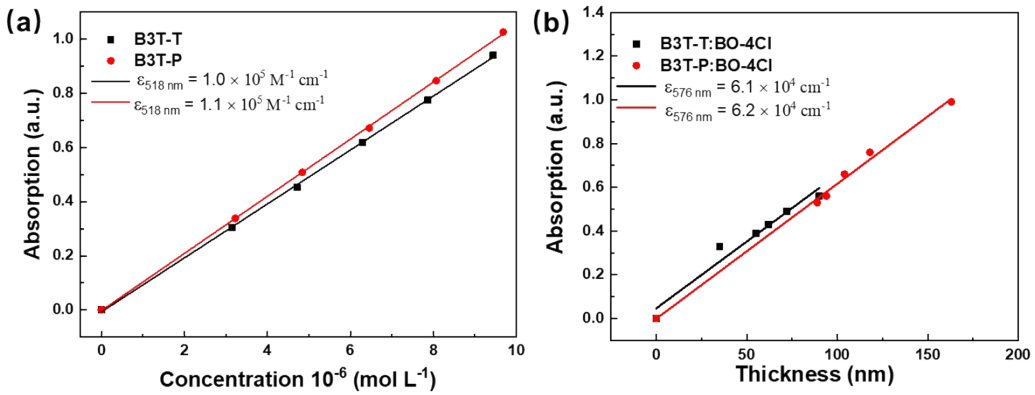

Figure S2. Extinction coefficients calculated from the absorption (a) at 518 nm plot dependent-concentration at room temperature for both small molecule donors, (b) at 576 nm plot dependent-thickness at room temperature for both blend films.

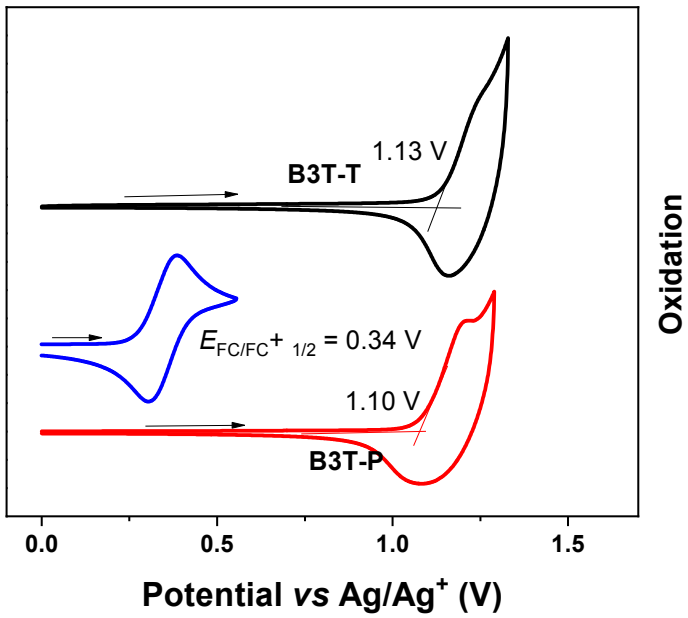

Figure S3. The oxidiation and reduction profiles of **B3T-T** and **B3T-P**.

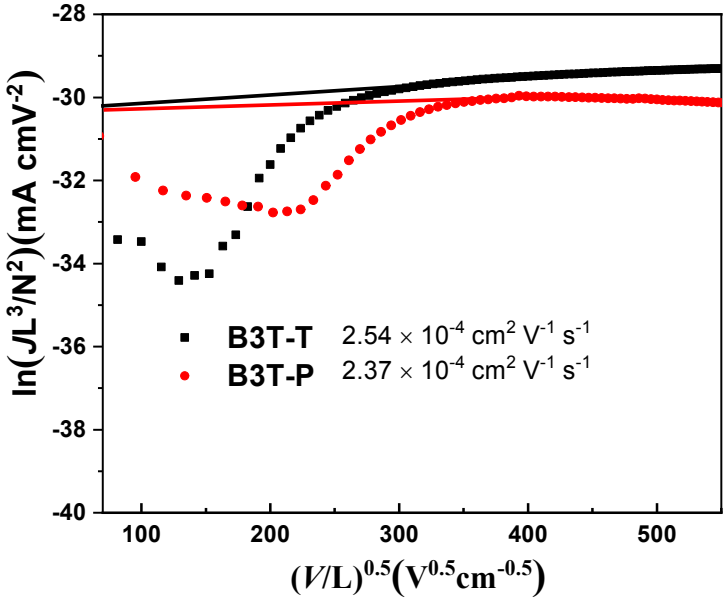

Figure S4. Plots for the calculation of hole mobilities of the neat **B3T-T** and **B3T-P** films obtained from the hole-only devices.

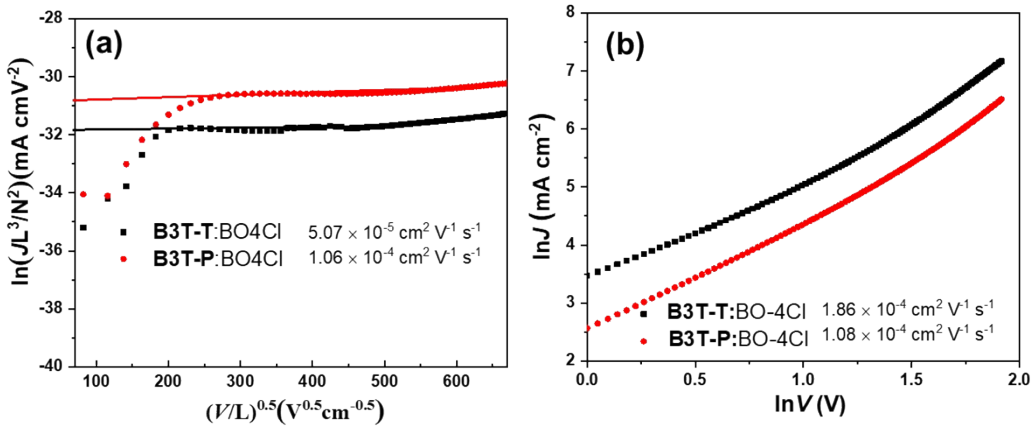

Figure S5. Plots for the calculation of hole and electron mobilities of **B3T-T**:BO-4Cl and **B3T-P**:BO-4Cl film obtained from the (a) hole-only and (b) electron-only devices.

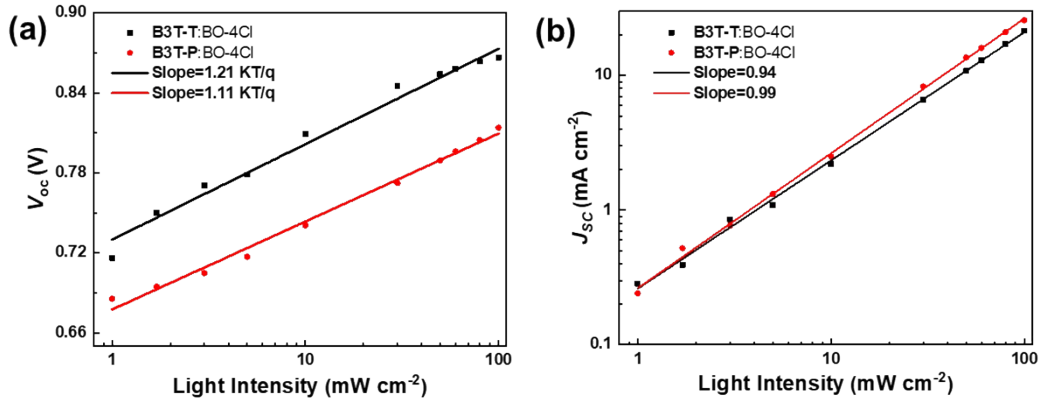

Figure S6. The light intensity versus (a) V_{OC} and (b) J_{SC} curves of the **B3T-T**:BO-4Cl- and **B3T-P**:BO-4Cl-based SM-OSCs

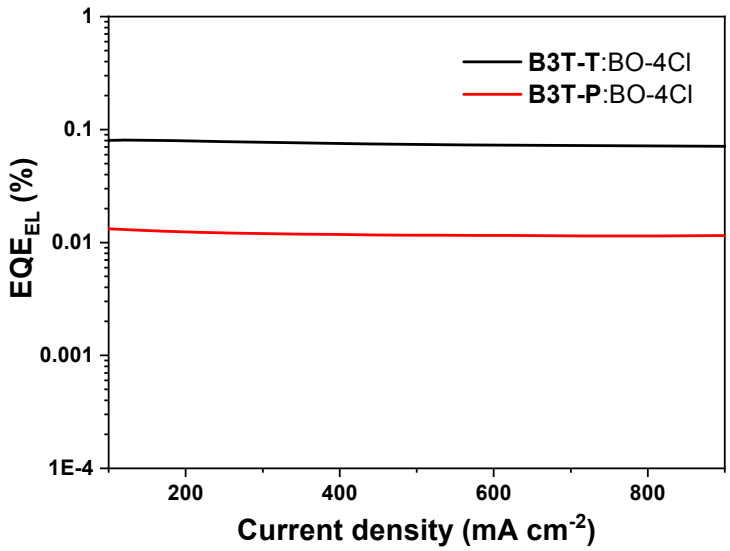

Figure S7. EQE_{EL} spectra of **B3T-T**- and **B3T-P**-based devices.

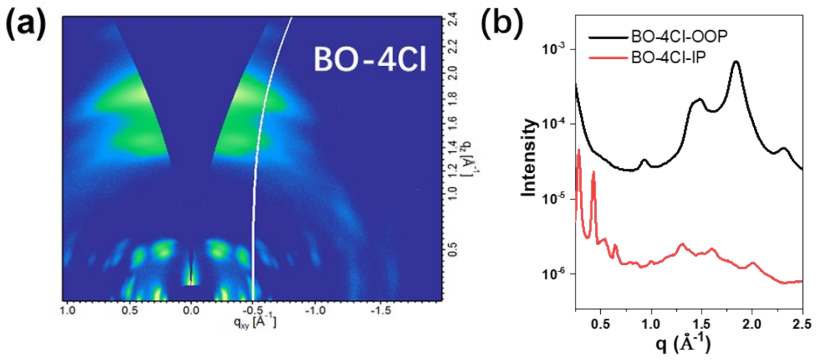

Figure S8. (a) GIWAXS patteren of BO-4Cl;(b) GIWAXS profile of BO-4Cl.

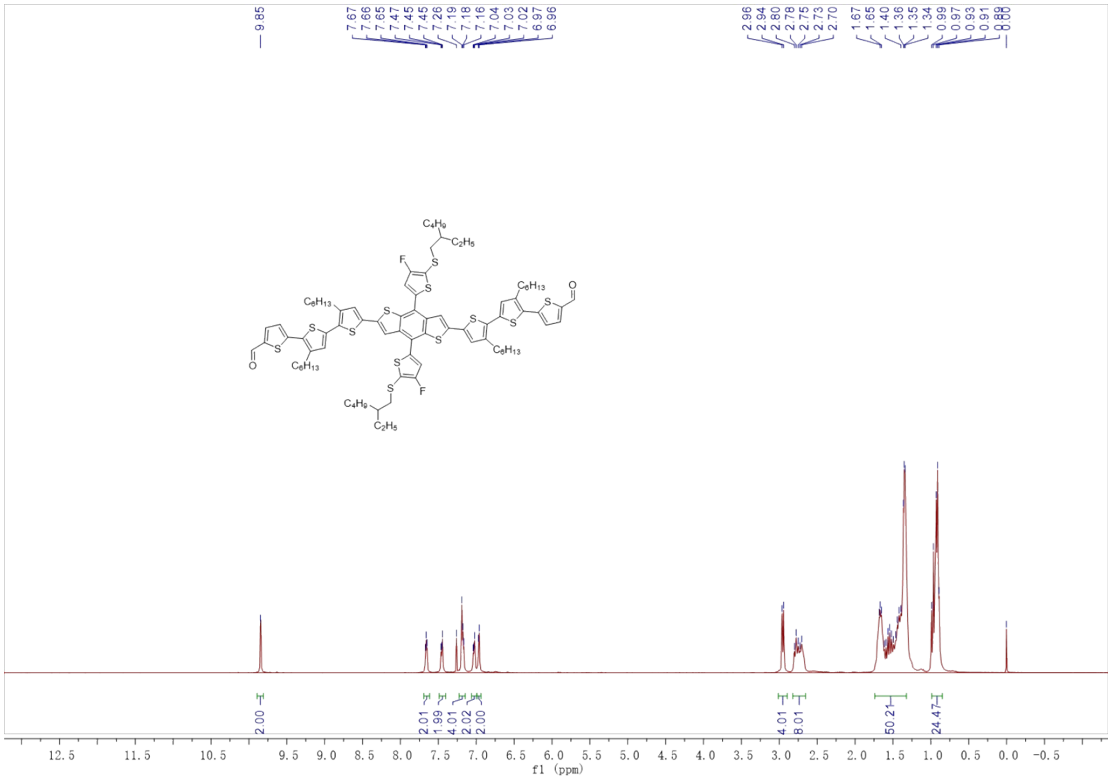

Figure S9. 1H-NMR spectra of compound **3a** in $CDCl_3$.

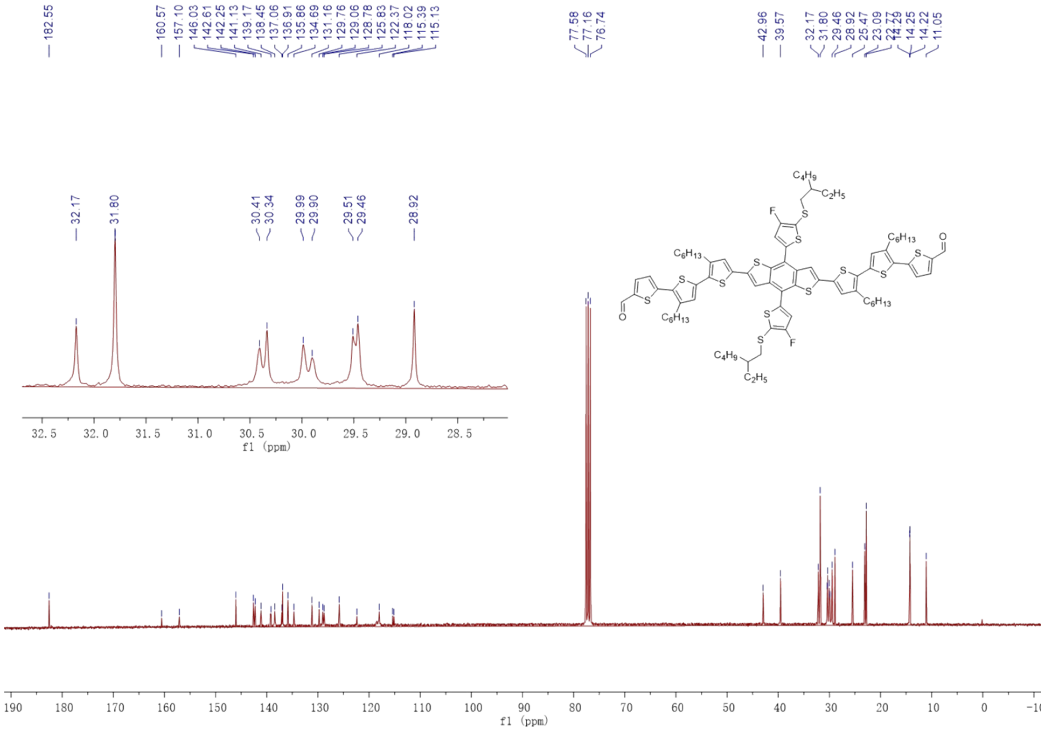

Figure S10 ^{13}C-NMR spectra of compound **3a** in $CDCl_3$.

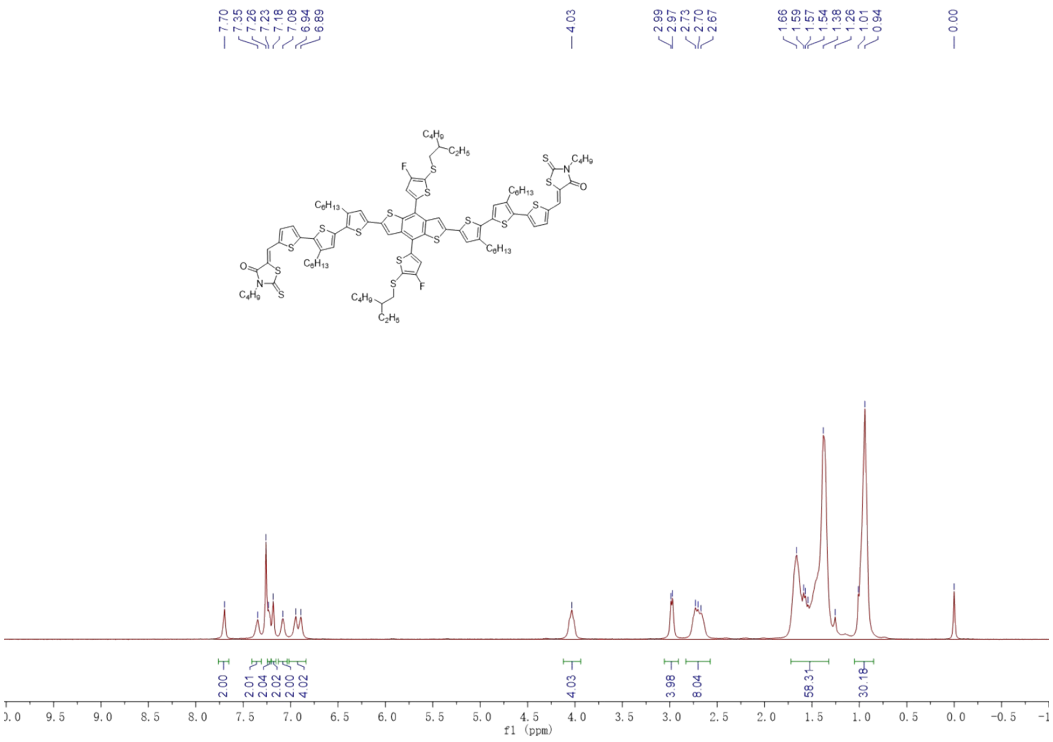

Figure S11. 1H-NMR spectra of compound **B3T-T** in $CDCl_3$.

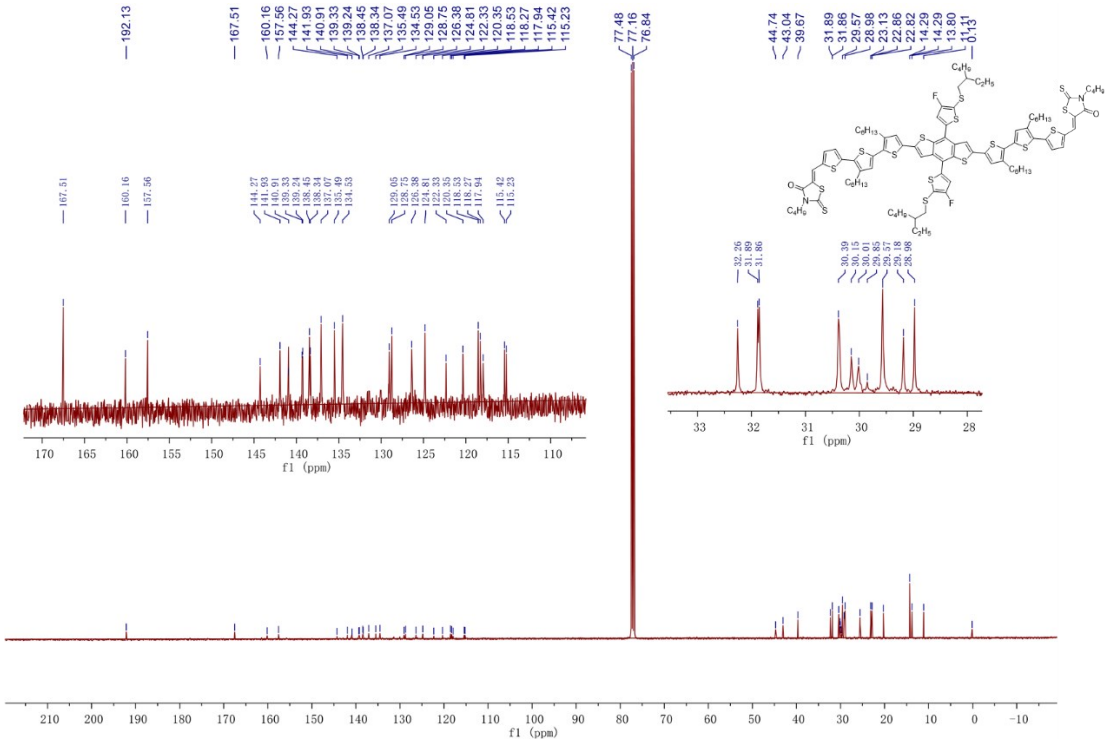

Figure S12 ^{13}C-NMR spectra of compound **B3T-T** in $CDCl_3$.

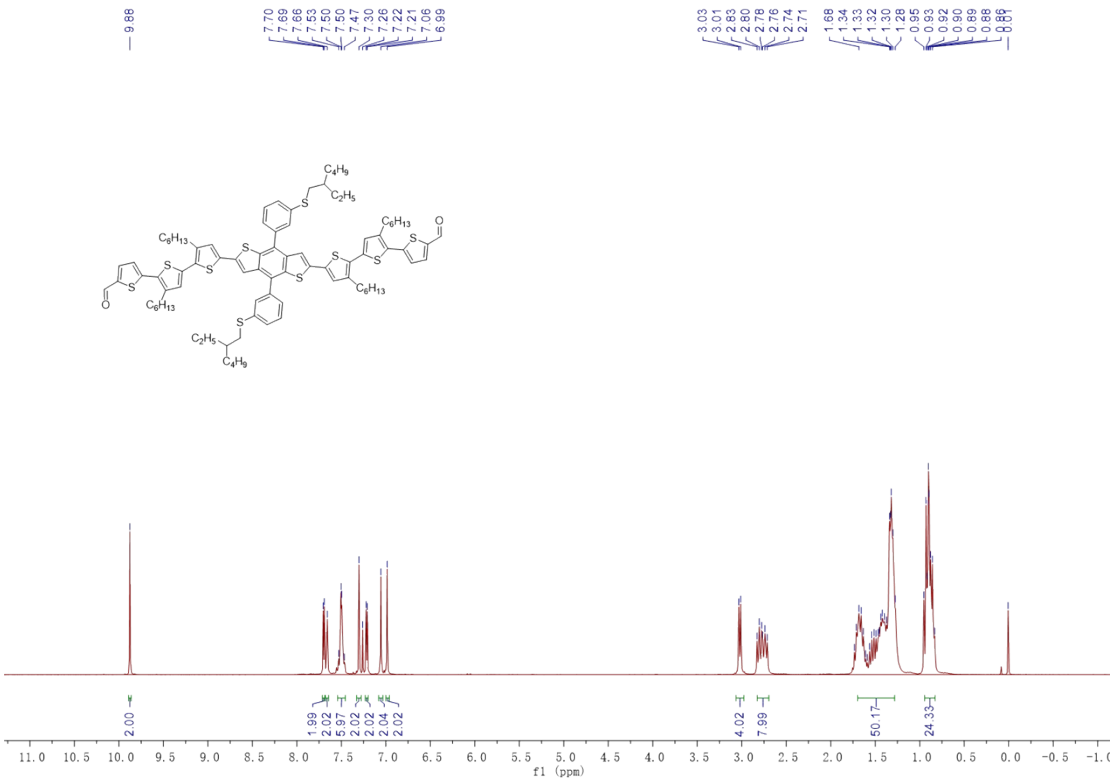

Figure S13. 1H-NMR spectra of compound **3b** in $CDCl_3$.

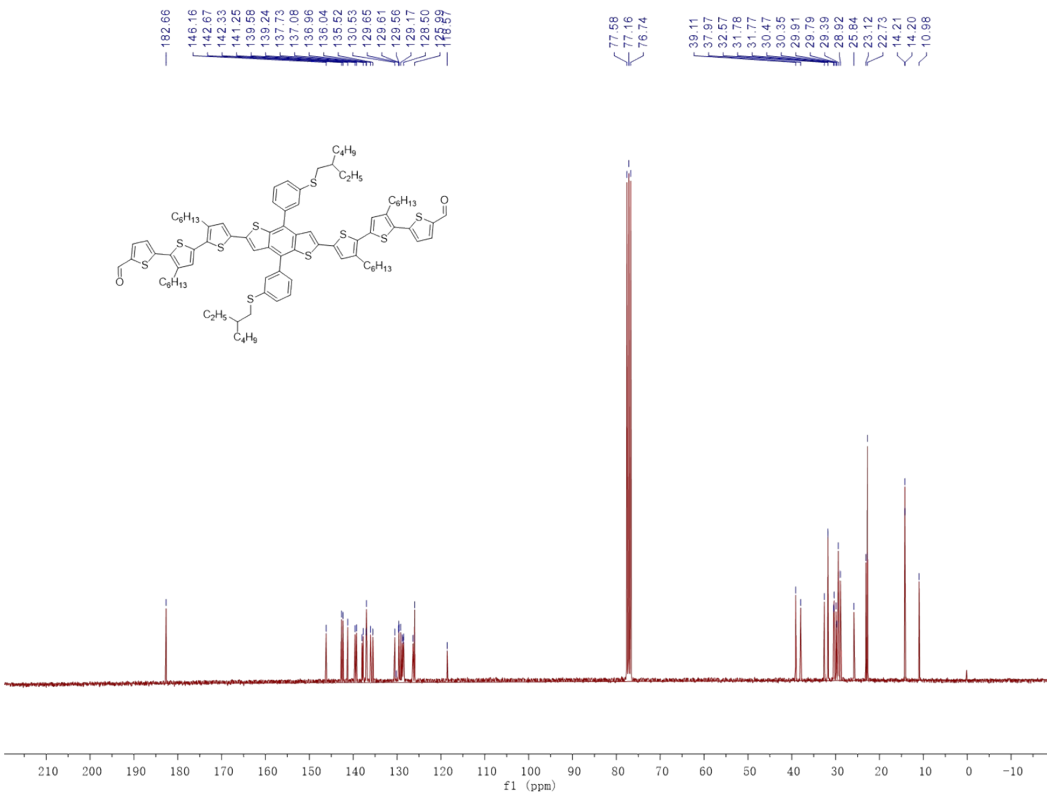

Figure S14 ^{13}C-NMR spectra of compound **3b** in $CDCl_3$.

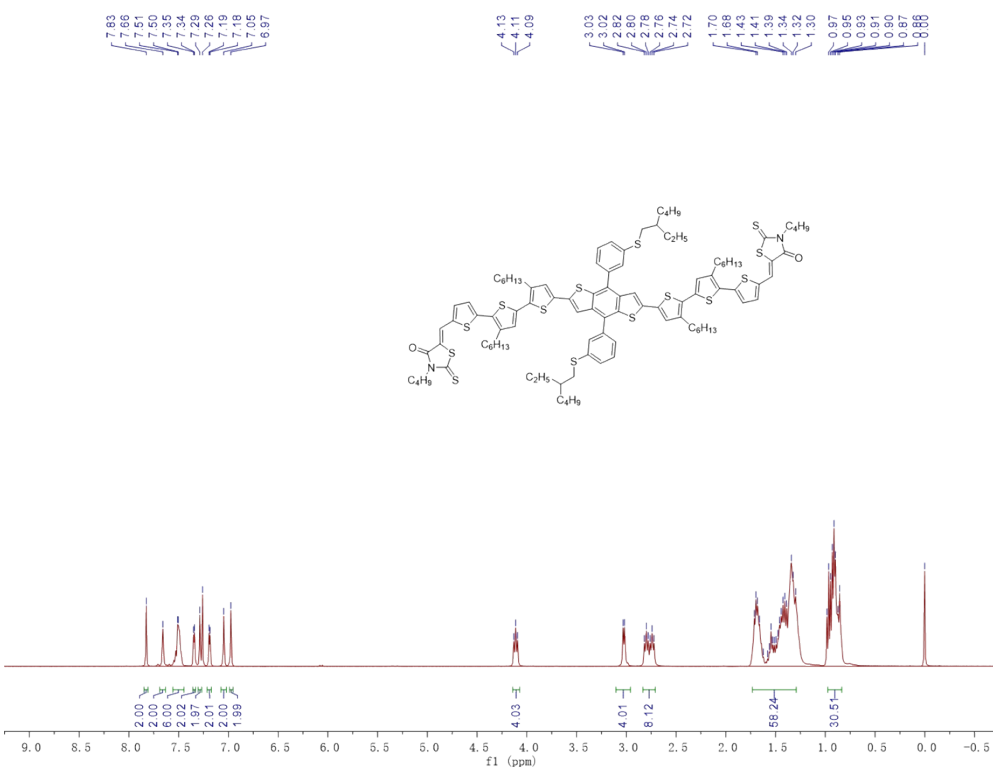

Figure S15. 1H-NMR spectra of compound **B3T-P** in $CDCl_3$.

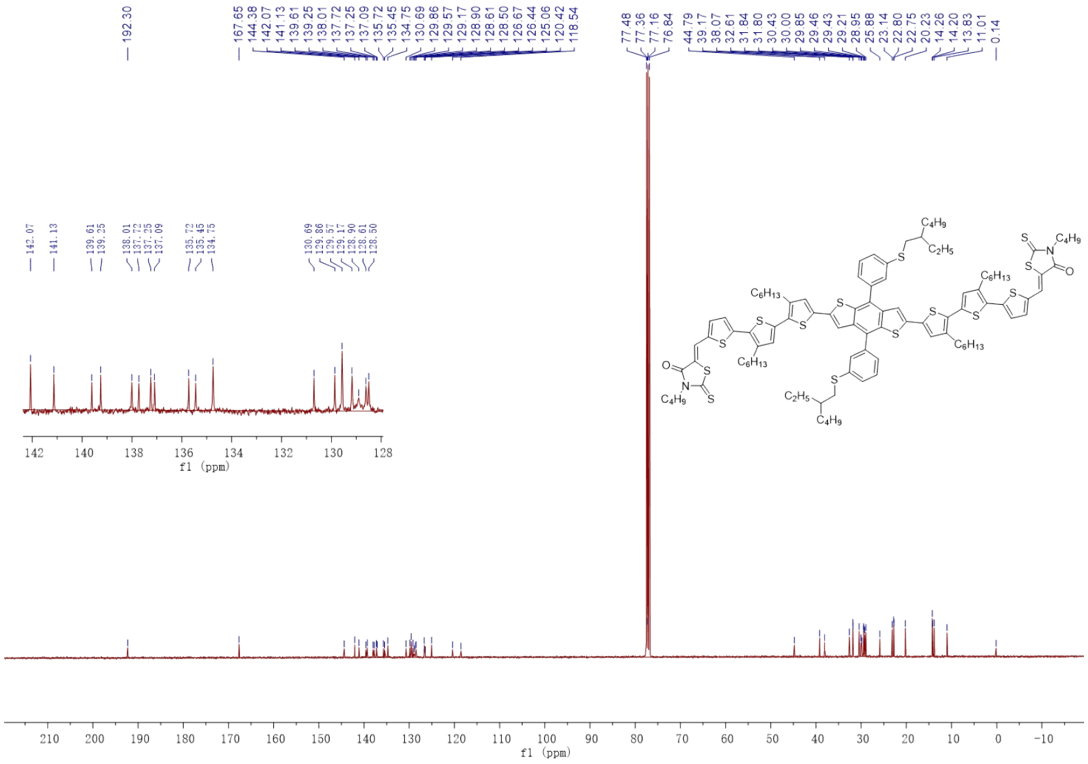

Figure S16 ^{13}C-NMR spectra of compound **B3T-P** in $CDCl_3$.

Table S1. Summary of photovoltaic parameters for the best PCE of the **B3T-T**:BO-4Cl-based SMOSCs with different chlorobenzene annealing time under simulated AM 1.5 G (100 mW cm^{-2}) illumination.[(a)]

Annealing time	V_{OC} (V)	J_{SC} (mA cm^{-2})	FF	*PCE* (%)
0	0.925	3.2	0.300	0.9
45	0.875	21.7	0.557	10.6
50	0.868	22.08	0.566	10.8
55	0.867	21.9	0.582	11.1
60	0.863	18.84	0.617	10.0

[(a)] **B3T-T**:BO-4Cl (1:1 w/w) were dissolved in chloroform solution with a total concentration of 20 mg mL^{-1}. The solution was heated to 40 °C. The resulting solution was spin-coated onto PEDOT:PSS modified ITO in succession. The thickness (around 100 nm) of film was controlled the spin-coating speed at 2000-3000 r.m.p. Subsequently, the active layer was annealed using chlorobenzene.

Table S2. Summary of photovoltaic parameters for the best PCE of the **B3T-T**:BO-4Cl-based SMOSCs with different D:A ratio under simulated AM 1.5 G (100 mW cm^{-2}) illumination.[(a)]

DIO ratio	V_{OC} (V)	J_{SC} (mA cm^{-2})	FF	*PCE* (%)
1.2:1	0.865	16.9	0.652	9.5
1:1	0.867	21.9	0.582	11.1
1:1.2	0.865	19.9	0.581	10.0

[(a)] **B3T-T**:BO-4Cl with different weight ratio were dissolved in chloroform solution with a total concentration of 20 mg mL^{-1}. The solution was heated to 40 °C until total dissolution. The resulting solution was spin-coated onto PEDOT:PSS modified ITO in succession. The thickness (around 100 nm) of film was controlled the spin-coating speed at 2000-3000 r.m.p. Subsequently, the active layer was annealed using chlorobenzene solvent for 55 second.

Table S3. Summary of photovoltaic parameters for the best PCE of the **B3T-T**:BO-4Cl-based SMOSCs with different D:A ratio under simulated AM 1.5 G (100 mW cm^{-2}) illumination.[(a)]

Thickness	V_{OC} (V)	J_{SC} (mA cm^{-2})	FF	*PCE* (%)
80	0.865	18.38	0.612	9.7
105	0.867	21.9	0.582	11.1
133	0.882	20.87	0.594	10.9
162	0.878	21.81	0.476	9.1
225	0.863	20.16	0.493	8.6

[(a)] **B3T-T**:BO-4Cl with different weight ratio were dissolved in chloroform solution with a total concentration of 20 mg mL^{-1}. The solution was heated to 40 °C until total dissolution. The resulting solution was spin-coated onto PEDOT:PSS modified ITO in succession. The thickness of film was controlled the spin-coating speed at 1500-3500 r.m.p. Subsequently, the active layer was annealed using chlorobenzene solvent for 55 second.

Table S4. Summary of photovoltaic parameters for the best PCE of the **B3T-P**:BO-4Cl-based SMOSCs with different chlorobenzene annealing time under simulated AM 1.5 G (100 mW cm^{-2}) illumination.[(a)]

Annealing time	V_{OC} (V)	J_{SC} (mA cm^{-2})	FF	*PCE* (%)
0	0.899	3.5	0.305	1.0
45	0.832	22.7	0.486	9.2
50	0.812	25.6	0.693	14.4
55	0.815	25.7	0.724	15.2
60	0.806	24.2	0.708	13.8

[(a)] **B3T-P**:BO-4Cl (1:1 w/w) were dissolved in chloroform solution with a total concentration of 20 mg mL^{-1}. The solution was heated to 40 °C. The resulting solution was spin-coated onto PEDOT:PSS modified ITO in succession. The thickness (around 100 nm) of film was controlled the spin-coating speed at 2000-3000 r.m.p. Subsequently, the active layer was annealed using chlorobenzene.

Table S5. Summary of photovoltaic parameters for the best PCE of the **B3T-P**:BO-4Cl-based SMOSCs with different D:A ratio under simulated AM 1.5 G (100 mW cm^{-2}) illumination.[(a)]

DIO ratio	V_{OC} (V)	J_{SC} (mA cm^{-2})	FF	*PCE* (%)
1.2:1	0.806	23.4	0.744	14.0
1:1	0.815	25.7	0.724	15.2
1:1.2	0.804	24.6	0.678	13.4

[(a)] **B3T-P**:BO-4Cl with different weight ratio were dissolved in chloroform solution with a total concentration of 20 mg mL^{-1}. The solution was heated to 40 °C until total dissolution. The resulting solution was spin-coated onto PEDOT:PSS modified ITO in succession. The thickness (around 100 nm) of film was controlled the spin-coating speed at 2000-3000 r.m.p. Subsequently, the active layer was annealed using chlorobenzene solvent for 55 second.

Table S6. Summary of photovoltaic parameters for the best PCE of the **B3T-P**:BO-4Cl-based SMOSCs with different D:A ratio under simulated AM 1.5 G (100 mW cm^{-2}) illumination.[(a)]

Thickness	V_{OC} (V)	J_{SC} (mA cm^{-2})	FF	*PCE* (%)
85	0.812	24.75	0.685	13.8
102	0.815	25.70	0.724	15.2
131	0.814	25.55	0.701	14.6
182	0.806	24.47	0.682	12.7
265	0.804	24.76	0.593	11.8

[(a)] **B3T-P**:BO-4Cl with different weight ratio were dissolved in chloroform solution with a total concentration of 20 mg mL^{-1}. The solution was heated to 40 °C until total dissolution. The resulting solution was spin-coated onto PEDOT:PSS modified ITO in succession. The thickness of film was controlled the spin-coating speed at 1500-3500 r.m.p. Subsequently, the active layer was annealed using chlorobenzene solvent for 55 second.

Table S7. The key GIWAXS data for **B3T-T**, **B3T-P**, BO-4Cl, and blend films

materials	100 / nm	200 / nm	300 / nm	010 / nm	CL of π-π stacking /nm
B3T-T (OOP)	17.99 (0.349 $Å^{-1}$)	9.01 (0.697 $Å^{-1}$)	6.03 (1.04 $Å^{-1}$)		
B3T-T (IP)				0.36 (1.74 $Å^{-1}$)	6.68
B3T-P (OOP)	18.36 (0.342 $Å^{-1}$)	9.18 (0.684 $Å^{-1}$)	6.15 (1.02 $Å^{-1}$)		
B3T-P (IP)				0.36 (1.74 $Å^{-1}$)	6.47
BO-4Cl (OOP)				0.34 (1.84 $Å^{-1}$)	6.04
B3T-T:BO-4Cl (OOP)				0.35 (1.81$Å^{-1}$)	3.88
B3T-P:BO-4Cl (OOP)				0.34 (1.83 $Å^{-1}$)	5.66